JACS
JOURNAL OF THE AMERICAN CHEMICAL SOCIETY
Article
pubs.acs.org/JACS

Penetrating the Elusive Mechanism of Copper-Mediated Fluoromethylation in the Presence of Oxygen through the Gas-Phase Reactivity of Well-Defined $[LCuO]^+$ Complexes with Fluoromethanes ($CH_{(4-n)}F_n$, $n = 1-3$)

Nicole J. Rijs,*[,†] Patricio González-Navarrete,[‡] Maria Schlangen,[‡] and Helmut Schwarz*[,‡]

[‡]Institut für Chemie, Technische Universität Berlin, Straße des 17. Juni 115, 10623 Berlin, Germany

[†]Institute of Nanotechnology, Karlsruhe Institute of Technology, Hermann-von-Helmholtz Platz 1, 76344 Eggenstein-Leopoldshafen, Germany

Supporting Information

ABSTRACT: Traveling wave ion mobility spectrometry (TWIMS) isomer separation was exploited to react the particularly well-defined ionic species $[LCuO]^+$ (L = 1,10-phenanthroline) with the neutral fluoromethane substrates $CH_{(4-n)}F_n$ ($n = 1-3$) in the gas phase. Experimentally, the monofluoromethane substrate ($n = 1$) undergoes both hydrogen-atom transfer, forming the copper hydroxide complex $[LCuOH]^{\bullet+}$ and concomitantly a $CH_2F^{\bullet}$ radical, and oxygen-atom transfer, yielding the observable ionic product $[LCu]^+$ plus the neutral oxidized substrate $[C,H_3,O,F]$. DFT calculations reveal that the mechanism for both product channels relies on the initial C−H bond activation of the substrate. Compared to nonfluorinated methane, the addition of fluorine to the substrate assists the reactivity through a lowering of the C−H bond energy and reaction preorganization (through noncovalent interaction in the encounter complex). A two-state reactivity scenario is mandatory for the oxidation, which competitively results in the unusual fluoromethanol product, CH_2FOH, or the decomposed products, CH_2O and HF, with the latter channel being kinetically disfavored. Difluoromethane ($n = 2$) is predicted to undergo the analogous reactions at room temperature, although the reactions are less favored than those of monofluoromethane. The reaction of trifluoromethane ($n = 3$, fluoroform) through C−H activation is kinetically hindered under ambient conditions but might be expected to occur in the condensed phase upon heating or with further lowering of reaction barriers through templation with counterions, such as potassium. Overall, formation of $CH_{(3-n)}F_n^{\bullet}$ and $CH_{(3-n)}F_nOH$ occurs under relatively gentle energetic conditions, which sheds light on their potential as reactive intermediates in fluoromethylation reactions mediated by copper in the presence of oxygen.

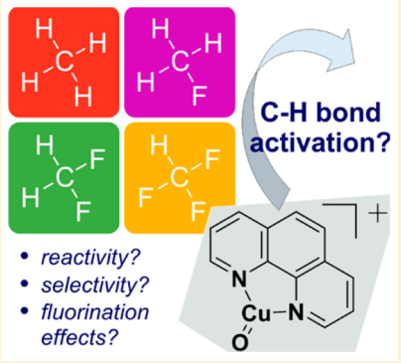

INTRODUCTION

Driven by the usefulness of fluorinated methyl groups in modulating physical properties, physiological availability, and stability in a wide range of applications,[1−6] great efforts have been made toward the selective fluoromethylation of organic substrates, in particular, trifluoromethylation.[7−9] Because of the monetary and environmental expense of other substrates, such as CF_3I,[10] fluoromethanes (e.g., fluoroform) are viewed as an attractive set of feedstocks to provide a source of fluorinated methyl groups.[11,12] Reaction conditions must be mild enough that the desirable fluoromethyl group, $-CH_{(3-n)}F_n$ ($n = 1-3$), can be delivered intact to the organic framework, without significant decomposition through fluorocarbenes or HF. For example, the generation of $CF_3^{\bullet}$ radicals in a controlled manner using metal catalysts allows these radicals to be introduced in aryl trifluoromethylations.[13−16]

Grushin and co-workers recently showed that copper species can effectively mediate fluoromethylation reactions in the condensed phase utilizing the cheap fluorocarbon substrate fluoroform to generate "$CuCF_3$"[17,18] and that the presence of oxygen is often crucial in promoting the reaction.[19] Despite continued efforts to study the isolated reactive species and intermediates, well-defined active species remain elusive; however, free CF_3^- and CF_3^+ have been excluded from being involved. In a combined computational/experimental study, it was revealed that a cooperative mechanism involving the potassium counterion as a templating agent (Scheme 1) allows C−H bond activation to occur at an oxygen center, which accounts for the cupration of fluoroform, CHF_3.[20]

For inert substrates, metal oxide catalysts often allow desirable bond activation reactions to occur under ambient conditions and improved selectivity.[21−23] After having been theoretically predicted to be particularly suited to the task,[24] many copper oxide catalysts have been developed for the C−H bond activation of methane,[25−35] and it is also understood that enzymes such as particulate methane monooxygenase (pMMO) utilize copper active sites for the same function,

Received: December 11, 2015
Published: February 9, 2016

DOI: 10.1021/jacs.5b12972
J. Am. Chem. Soc. 2016, 138, 3125−3135

Scheme 1. Predicted Transition State for the Cupration of Fluoroform Brought about by C−H Bond Activation, Assisted by "Templation" Provided by the Potassium Counterion, K[a]

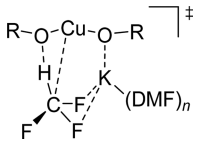

[a]Adapted from ref 20.

with O_2 as the terminal oxidant.[36] However, as substrates in metal-mediated reactions, the chemistry of fluorinated aliphatic compounds is not yet as thoroughly understood as that of their purely hydrocarbon counterparts, where decades of mechanistic research has provided solid principles for C−H bond activations, for example, through the gas-phase study of the hydrogen-atom transfer (HAT) reactions of methane,[37−42] for which there are many recent examples.[43−58] The inclusion of fluorine in metal-mediated reactions inherently changes the reactivity;[14,59,60] for example, cross-coupling efficiency can be diminished by the electron-withdrawing capacity of fluoro groups in activation complexes.[61] In other cases, selectivity can be reversed; for example, in the organocuprate-mediated coupling reaction with allyl iodide, fluorination of the substrate leads to stabilization of the Cu(III) intermediate and a different reaction product (homocoupling versus cross-coupling).[62,63] Thus, standard synthetic procedures for hydrocarbon substrates are not always directly transferable to their fluorinated counterparts.

Gas-phase reactions of mass-selected ionic species can provide a wealth of information on the local bond-breaking or -making events that are often obscured in the complex condensed-phase environment, such as that present in homogeneous catalysis.[64] Gas-phase information alone, however, cannot replace that of condensed-phase provenance, where solvent and counterions are often key to the overall reactivity. Nonetheless, when this gas-phase information is used in combination with electronic structure calculations, one can generate a solid base of mechanistic principles.[65−68] By first understanding the intrinsic unit, the bottom-up development of catalysts and chemical reactions in the complex condensed-phase environment becomes more feasible.[66−72]

Copper-oxo intermediates serve as likely reactive species in copper-mediated reactions with radical-like behavior occurring in the presence of oxygen, such as those described above. In general, the role played by the degree of fluorination in metal-mediated reactions is poorly understood and warrants systematic study,[73−75] along with the selectivity for C−H versus C−F bond activations.[76] The formation of $CH_{(3-n)}F_n^{\bullet}$ radicals in a controlled manner such that the methyl group remains intact[13−16] (i.e., is not degraded into fluorocarbenes, as is often the mechanistic case for methods that require heating[77,78]) is a highly desirable process to understand. Thus, here we seek to both (1) systematically understand the process of C−H bond activation of fluoromethane substrates $CH_{(3-n)}F_n$ (n = 1−3) and compare it with that of methane and (2) discover whether $CuCF_3$ and analogous fluorinated copper species can be generated in the absence of a templating counterion, to unravel the mechanistically more complex behaviors.[77,79,80] We aim to gain insight into the reactions through the very well-defined copper and copper-oxo complexes (Scheme 2, **1**−**3**) isolated in the gas phase.[81−84]

Scheme 2

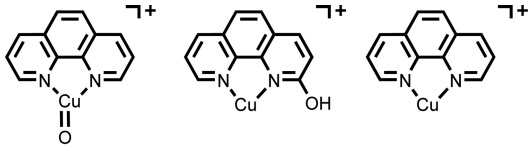

1 **2** **3**

Isomers **1** and **2** have been experimentally characterized extensively, by means of collision-induced dissociation (CID), ion mobility, and infrared multiphoton dissociation (IRMPD).[82−84] In addition, their gas-phase reactivities have been explored.[81−85] Briefly, complex **1** was found to activate various aliphatic and aromatic C−H bonds, such as propane and benzene; however, it is unable to activate those of methane.[81−85] The related diatomic complex, $[CuO]^+$, in contrast, is able to activate methane under ambient condtions.[24,86,87] As the complexes (formed by ESI of nitrate salts and ligand) have been extensively characterized[82−84] and are thus well-defined, we focus herein on their reaction with fluoromethanes, $CH_{(3-n)}F_n$ (n = 1−3).

RESULTS AND DISCUSSION

Experimental Results. The copper and copper-oxo species (Scheme 2, **1** and **2**) were cogenerated from a methanolic solution of 1,10-phenanthroline and copper(II) nitrate introduced into the mass spectrometer through the ESI source, as previously described.[82−84] The mass-selected ^{63}Cu-containing species at m/z 259 were subsequently separated by traveling-wave ion-mobility spectrometry (TWIMS), as also previously described.[84] Complex **3** (Scheme 2, m/z 243) was generated in the same manner and simply mass-selected. Utilizing instrumental modifications, ion/molecule reactions can be optionally carried out in the "trap"[88] and "transfer cell",[84] the regions represented schematically in Scheme 3. Gas-phase ion/molecule reactions between the fluoromethanes and the well-defined copper species were carried out in this work in the transfer cell, using both the standard sequential processes within the hybrid instrument, along with the aforementioned modifications.[84,89]

Thus, gaseous fluoromethanes ($CH_{(4-n)}F_n$, n = 1−4) were leaked into the transfer cell at various pressures and allowed to react during the time frame of transit through the transfer region (0.57 ms).[90] The fluoromethanes reacted with copper complexes **2** and **3** through monofluorocarbene (Supporting Information, Figures S1 and S2) and did not result in the retention of an intact methyl group; therefore, we focus on the ion/molecule reactions of **1**. The resulting mass spectra of the isolated reactive copper-oxo species **1** (i.e., no neutral substrate), along with the reactions of **1** with $CH_{(4-n)}F_n$, n = 1−3, are detailed in panels a−d, respectively, of Figure 1. CF_4 was found to be completely unreactive with all of the copper complexes generated and, thus, is not discussed further.

Consistent with previous results,[82,84] even without addition of a neutral substrate, the background water present within the instrument is able to react with **1**, resulting in the H_2O adduct $[(phen)CuO(H_2O)]^+$ and a hydrogen-atom abstraction product, the copper-hydroxo complex $[(phen)CuOH]^{\bullet+}$, forming the major peak at m/z 277 and a minor peak at m/z 260,

DOI: 10.1021/jacs.5b12972
J. Am. Chem. Soc. 2016, 138, 3125−3135

Scheme 3. Experimental Setup of the Modified Synapt-G2 Mass Spectrometer

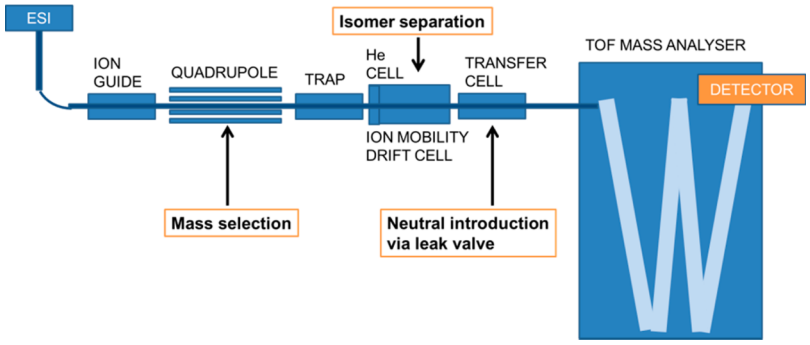

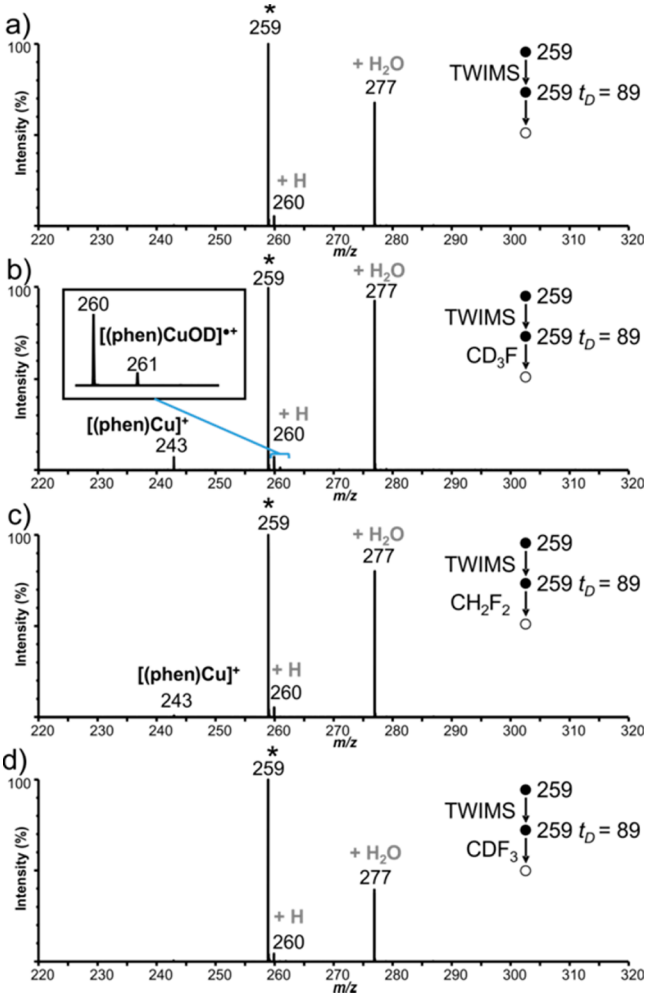

Figure 1. ESI-TWIMS-MS spectra after separation of **1**, $[(phen)CuO]^+$: (a) with only argon, no neutral substrate introduced through the leak valve; (b) reacting with CD_3F at a pressure of 3×10^{-3} mbar; (c) reacting with CH_2F_2 at a pressure of 3×10^{-3} mbar; (d) reacting with CDF_3 at a pressure of 2×10^{-2} mbar. The mass-selected ion in each spectrum is denoted by an asterisk (*), and the drift time (t_D) is given in bins. Products due to reaction with background molecules are labeled in gray. The ESI cone voltage was 40 V for each spectrum.

respectively (Figure 1a). Oxygen elimination is also observed in a minute abundance. This is unlikely to be due to fragmentation (eq 2b), as density functional theory (DFT) predicts the bond dissociation energy (BDE) of Cu−O to be +212 kJ mol^{-1}; therefore, it must also arise through reaction with background molecules.[82]

$$[(phen)CuO]^+ + CX_{(4-n)}F_n \longrightarrow [(phen)CuOX]^{\bullet+} + CX_{(3-n)}F_n^{\bullet} \quad (1)$$

$$X = H \text{ or } D \longrightarrow [(phen)Cu]^+ + COX_{(4-n)}F_n \quad (2a)$$

$$\longrightarrow [(phen)Cu]^+ + O + CX_{(4-n)}F_n \quad (2b)$$

Reacting **1** with monofluoromethane, CH_3F, results in a mass spectrum similar to that with the background only, except that oxygen-atom transfer (OAT) to the substrate is observed as indicated by the distinct signal at m/z 243 (eq 2a, X = H). The potential channel of HAT from the monofluoromethane substrate (eq 1) is obscured by the water reaction described above and in Figure 1a. Thus, perdeuterated monofluoromethane, CD_3F, was reacted to resolve the reactivity from that of the background (Figure 1b). Consistent with deuterium-atom transfer from CD_3F (eq 1, X = D), a peak at m/z 261 is observed (Figure 1b). OAT (eq 2a) is clearly discernible from background reactions (Figure 1a) by the high relative abundance of m/z 243 (Figure 1b). For example, even though the substrate pressure is the same in the two spectra depicted in Figure 1b and Figure 1c, the abundance is much higher in the former, indicative of an OAT reaction taking place.

In contrast, using the same pressure of neutral gas, reaction with CH_2F_2 results in a far lower yield of $[(phen)Cu]^+$ (Figure 1c), suggesting a lower propensity for OAT (eq 2a, X = H, n = 2). Unfortunately, the high cost of perdeuterated difluoromethane precludes it from experimental consideration; thus, CD_2F_2 was not reacted here. Therefore, it cannot be directly ascertained by experiment whether HAT occurs from this substrate.

Even though the reaction with deuterated fluoroform, CDF_3 (Figure 1d), is at a pressure an order of magnitude higher (2×10^{-2} mbar) than the previous experiments, no apparent reaction is observed. This indicates that, at the limit of our experiments, no reaction between copper-oxo complex **1** and fluoroform is observable.

Computational Results. The electronic structure of the ligated copper-oxo cation, **1**, has a triplet ground state ($^3A_2$) with C_{2v} symmetry.[83] In contrast, the singlet copper oxo-cation ($^1A_1$) is calculated here to be 95.3 kJ mol^{-1} higher in energy than the triplet, which is consistent with the electronic states previously found computationally for the ion,[82−84] and the related diatomic.[86,87] Thus, in the potential energy surfaces (PESs) reported herein, the triplet ground state ($^3A_2$) is the energy reference of the reactant ion, ^{3}**1** (where the superscript 3 denotes the triplet electronic state and geometry). The predictions of DFT calculations for each of the fluorinated substrates, $CH_{(4-n)}F_n$, n = 1−3, and methane (n = 0) are discussed below in light of the experimental findings.

DOI: 10.1021/jacs.5b12972
J. Am. Chem. Soc. 2016, 138, 3125−3135

The initial C−H activation of aliphatic hydrocarbons catalyzed by molecular "Cu−O" species can take place through "direct" HAT (Scheme 4).[53,86] An additional, "metal-mediated"

Scheme 4

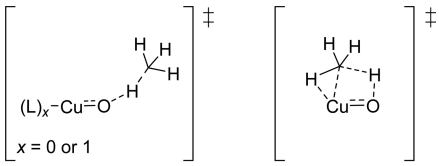

HAT mechanism of the type described by Ugalde and co-workers[87] for diatomic $[CuO]^+$ (Scheme 4) is not sterically possible for ^{3}**1**, because of the hindrance of the metal center imposed by the 1,10-phenanthroline ligand. Thus, we compare only the potential pathways resulting from direct HAT.

As noted above, unlike its diatomic $[CuO]^+$ counterpart,[86] the gas-phase cation ^{3}**1** does not experimentally react with methane at ambient conditions.[83,85] This is in agreement with the predicted kinetic barrier associated with a direct HAT process for methane (CH_4-^{3}**TS4−5**), which is 4.6 kJ mol^{-1} above the separated reactants, in contrast to the diatomic $[CuO]^+$, for which the barrier is ca. −7 kJ mol^{-1} below.[87] Thus, although the products of a reaction by eq 1 or eq 2a are exothermic overall, the C−H bond activation by HAT is kinetically inaccessible at room temperature for ^{3}**1**/CH_4. (For the full PES, see the Supporting Information, Figure S3.)

The direct HAT process as discussed for methane (Scheme 4) is also a potential pathway for the reactions of ^{3}**1** with fluoromethanes ($CH_{(4-n)}F_n$, n = 1−3). Incorporation of fluorine into the substrate lowers the bond energy of the C−H bonds compared to those in methane (Table 1, n = 1 and 2),

Table 1. Experimental Bond Energies (D°_{298}, kJ mol^{-1}) for $CH_{(4-n)}F_n$, n = 0−3, from the Literature[91]

n	bond	D°_{298}
0	H−CH_3	439.3 ± 0.4
1	H−CH_2F	423.8 ± 4.2
1	F−CH_3	460.2 ± 8.4
2	H−CHF_2	431.8 ± 4.2
2	F−CH_2F	496.2 ± 8.8
3	H−CF_3	445.2 ± 2.9
3	F−CHF_2	533.9 ± 5.9

which should kinetically and thermodynamically assist the direct HAT process, except in the case of fluoroform (n = 3).[91] Because of the polar nature of C−F bonds, there is also the potential for organization through fluorine interactions in the encounter and activation complexes, for example, as was shown in the heterobimetallic system detailed in Scheme 1.[20] As such organization can affect reactivity and selectivity, we also investigated the "template-assisted" mechanism (Scheme 5). In all cases (n = 1−3), it was found that a template-assisted (Scheme 5) geometry is lower in energy than a direct one.

Reaction of ^{3}1 with Monofluoromethane. The template-assisted HAT reaction of ^{3}**1** and CH_3F might occur through two pathways, path a and path b, which differ in the geometry of the templation occurring with respect to the 1,10-phenanthroline ligand (Figure 2). In path a, the templation proceeds with F out of the plane of the 1,10-phenanthroline

Scheme 5

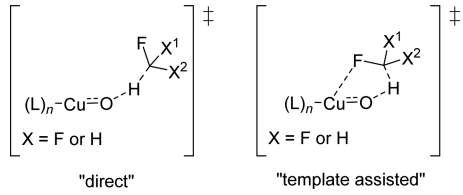

ligand, whereas for path b, the fluorine atom is in the plane. The exothermic and barrier-free formation of two possible encounter complexes (^{3}**4** and ^{3}**7** for out-of-plane and in-plane, respectively) occurs in a nonselective manner (each is ca. −26 kJ mol^{-1} below the energy of the separated reactants; Figure 2). Both ^{3}**4** and ^{3}**7** bind in an η^2 fashion, where the Cu center interacts with the F and the O ligand interacts with the H, with distances of d(Cu−F) = 2.483 and 2.196 Å and d(O−H) = 2.937 and 2.387 Å for ^{3}**4** and ^{3}**7**, respectively (Figure 3). From ^{3}**4** and ^{3}**7**, a direct abstraction of the hydrogen atom from CH_3F to the terminal oxygen might occur through ^{3}TS**4−5** or ^{3}TS**7−8**, respectively, resulting in the formation of the stable exothermic complexes ^{3}**5** or ^{3}**8**, in which the $CH_2F^\bullet$ radical is loosely coordinated to the corresponding copper hydroxide moiety (Figure 2). Whereas HAT by path a is accessible under thermal conditions with an activation energy of 16.4 kJ mol^{-1} (^{3}TS**4−5**; Figure 2), the large activation barrier (30.3 kJ mol^{-1}) resulting in an inaccessible transition state, ^{3}TS **7−8** (4.0 kJ mol^{-1} above the separated reactants; Figure 2), prevents path b from taking place. Therefore, the observed products ^{2}**10** ($[(phen)CuOH]^{\bullet+}$) and $CH_2F^\bullet$ (eq 1) are generated by path a according to the sequence: ^{3}**1** + CH_3F → ^{3}**4** → ^{3}TS**4−5** → ^{3}**5** → ^{2}**10** + $CH_2F^\bullet$. The overall spin-allowed HAT process is exothermic by 45 kJ mol^{-1} (Figure 2). The activation of CH_3F in the singlet electronic state has also been explored (Supporting Information, Figure S4). The C−H bond activation of CH_3F by ^{1}**1** through ^{1}TS**7−9** represents a proton-transfer mechanism. However, this proton transfer is predicted to be completely inaccessible under thermal conditions (138 kJ mol^{-1} above the separated reactants; Figure S4) and, therefore, does not play a role in the HAT observed. (For a discussion, please see the Supporting Information, page S7.)

Alcohol formation from intermediate ^{3}**5** on the spin-allowed triplet surface is not energetically feasible (Figure 2). Despite being compensated by a rather stable η^2-coordinated fluoromethanol product complex, ^{3}**6** (Figure 3), located −63.0 kJ mol^{-1} below the separated reactants, the transfer of the OH group from $[(phen)CuOH]^{\bullet+}$ toward the radical $CH_2F^\bullet$ through ^{3}TS**5−6** is associated with a large energy barrier of 75 kJ mol^{-1}. The segregation of the products ^{3}**3** and CH_2FOH is highly endothermic (inaccessible at 27 kJ mol^{-1} above the separated reactants). Hence, OAT from ^{3}**5** is kinetically and thermodynamically prevented on the spin-allowed triplet surface through path a.

As the spin-allowed OAT is not energetically feasible, instead, a two-state reactivity (TSR) scenario[92−96] is implicated in product formation through eq 2a. The generation of fluoromethanol under thermal conditions can only occur through intersystem crossing (ISC) from the triplet to the singlet surface. Once in the singlet state, the formation of fluoromethanol can take place in an energetically feasible manner, through a tight three-centered rebound TS (^{1}TS**9−6**;

DOI: 10.1021/jacs.5b12972
J. Am. Chem. Soc. 2016, 138, 3125−3135

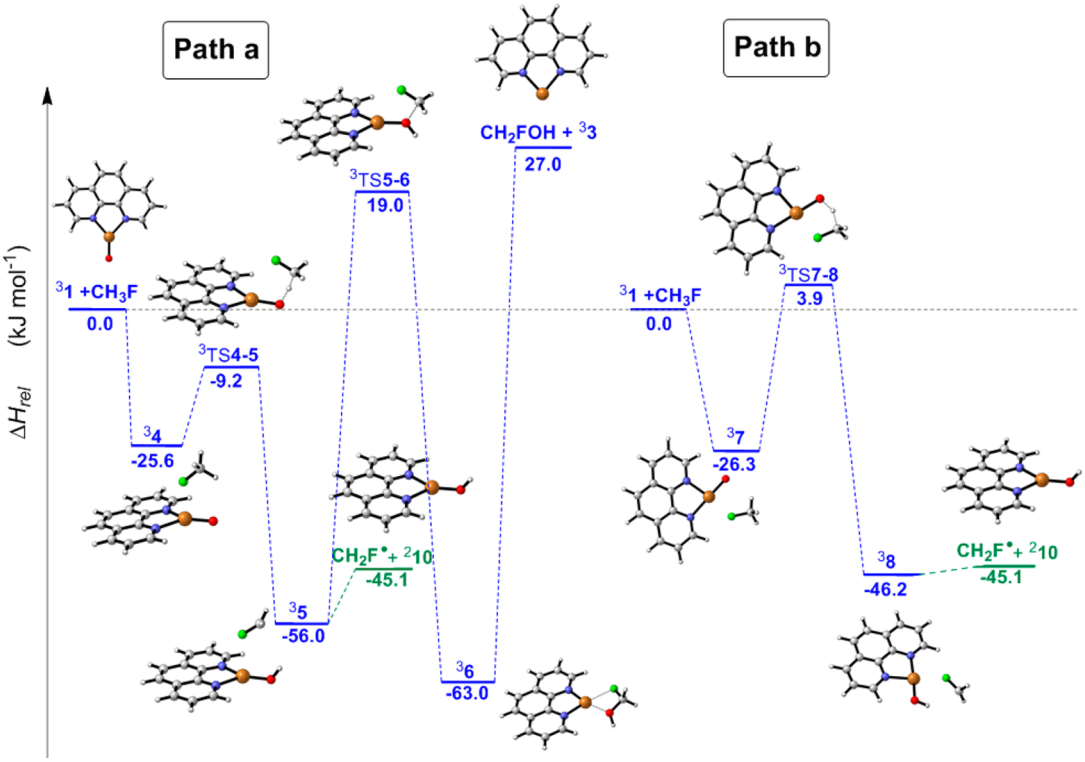

Figure 2. Relative enthalpies ΔH_{rel} (kJ mol^{-1}) for the reaction of $[(phen)CuO]^+$ with CH_3F. Optimization, frequencies, and energies were calculated using the B3LYP/TZVP+G(3df,2p):6-311++G(3df,2p) level of theory. (See Experimental Methods for basis-set definition.)

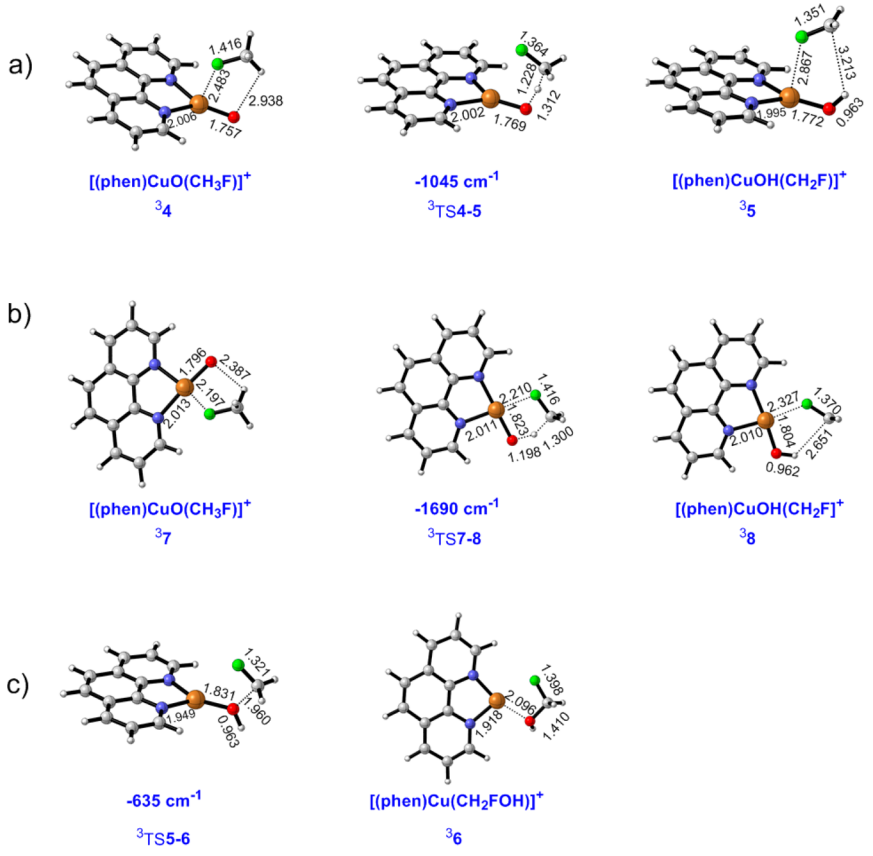

Figure 3. Minima optimized at the B3LYP/TZVP+G(3df,2p):6-311++G(3df,2p) level relevant for (a) HAT by path a, (b) HAT by path b, and (c) spin-allowed OAT. Only the electronic ground states are displayed for the reaction of $^3[(phen)CuO]^+$ with CH_3F. Bonds lengths are given in angstroms.

DOI: 10.1021/jacs.5b12972
J. Am. Chem. Soc. 2016, 138, 3125−3135

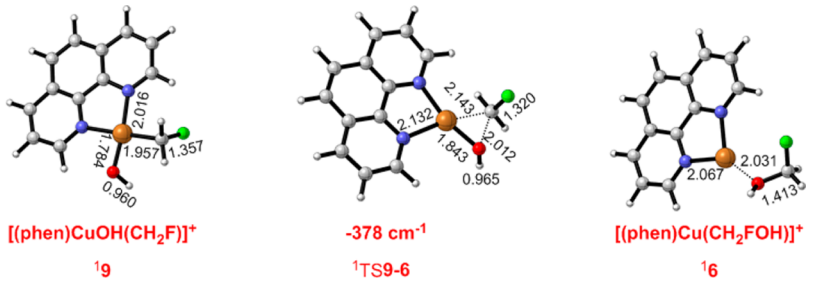

Figure 4. Minima relevant to the rebound step on the singlet surface optimized at the B3LYP/TZVP+G(3df,2p):6-311++G(3df,2p) level. Bonds lengths are given in angstroms.

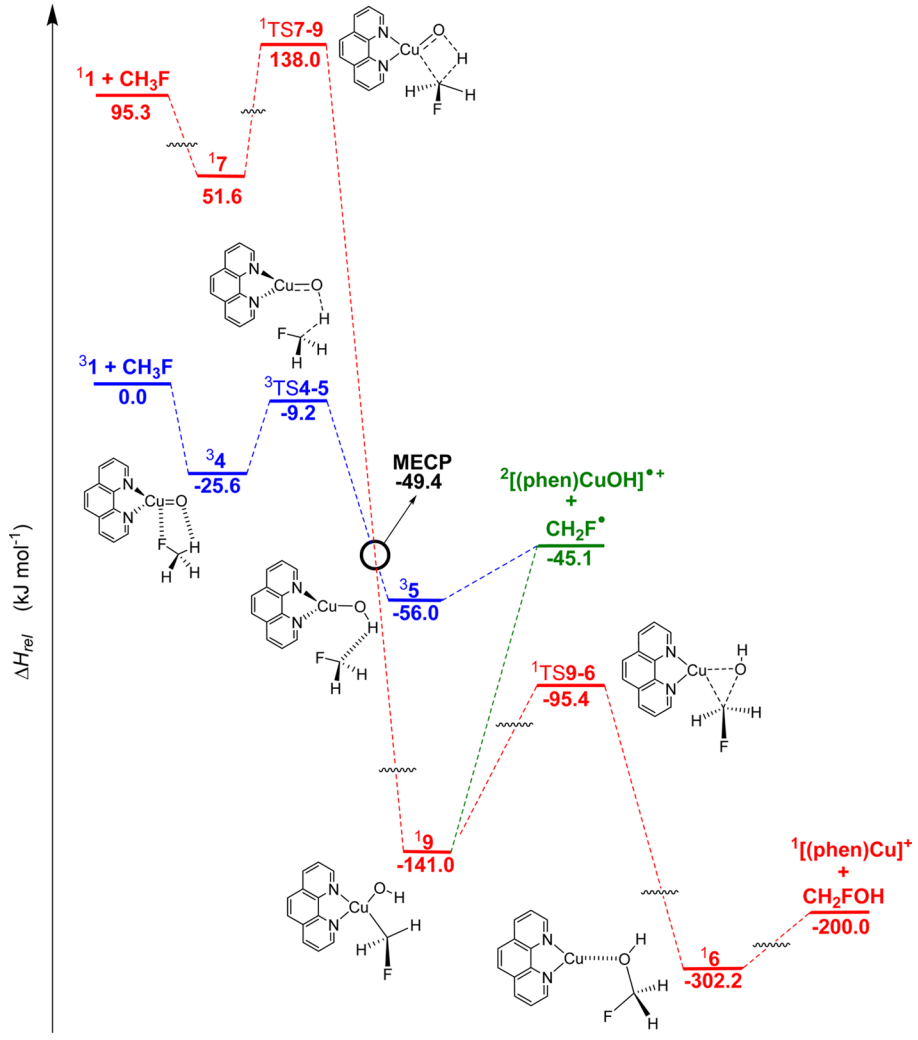

Figure 5. Mechanistic scenario for the reaction of $[(phen)CuO]^+$ with CH_3F [relative enthalpies, ΔH_{rel}, (kJ mol^{-1})]. Optimization, frequencies, and energies were calculated using the B3LYP/TZVP+G(3df,2p):6-311++G(3df,2p) level of theory. (See Experimental Methods for basis-set definition.)

Figure 4) that is −95.4 kJ mol^{-1} below the energy of the separated reactants (Figure 5).

A minimum-energy crossing point (MECP) on the seam line at which the singlet and triplet adiabatic surfaces intersect was located −49.4 kJ mol^{-1} below the energy of the separated reactants, positioned between ^{3}TS**4**−**5** and the copper-hydroxo complex ^{1}**9**. Thus, the formation of fluoromethanol proceeds through ISC according to the sequence ^{3}**1** + CH_3F → ^{3}**4** → ^{3}TS**4**−**5** → ISC → ^{1}**9** → ^{1}TS**9**−**6** → ^{1}**6** → ^{1}**3** + CH_2FOH, where the first stage is in common with the spin-allowed HAT process (Figure 5). Barrierless dissociation of the alcohol product is preferred over HF formation (Supporting Information, Figure S4).

Reactions of ^{3}1 with Di- and Trifluoromethane. In the reactions of copper-oxo species ^{3}**1** toward CH_2F_2 and CHF_3, the mechanistic scenarios are analogous to that of the ^{3}**1**/CH_3F system (Figure 5). Detailed PESs of the reaction of ^{3}**1** with both CH_2F_2 and CHF_3 are included in the Supporting Information (Figures S5 and S6, respectively). The corresponding HAT and OAT processes of CH_2F_2 and CHF_3 follow the same sequence as mentioned above for CH_3F; however,

DOI: 10.1021/jacs.5b12972
J. Am. Chem. Soc. 2016, 138, 3125−3135

Table 2. Activation Energies (E_a) and Relative Enthalpies Compared to the Separated Reactants (ΔH_{rel}) as Calculated[a] for the HAT (Triplet) and Oxygen-Atom Transfer (Singlet) Processes, as well as Dissociation Energies (D) of $CH_{(3-n)}F_n^{\bullet}$ (eq 1) and $CH_{(3-n)}F_nOH$ (eq 2a) for n = 0−3 (kJ mol^{-1})

		HAT (^{3}TS**4**−**5**)		MECP	^{1}**9**	rebound step (^{1}TS**9**−**6**)		^{2}**10** + $CH_{(3-n)}F_n^{\bullet}$ (eq1)		^{1}**3** + $CH_{(3-n)}F_nOH$ (eq2a)	
n		E_a	ΔH_{rel}	ΔH_{rel}	ΔH_{rel}	E_a	ΔH_{rel}	D(Cu−F)	ΔH_{rel}	D(Cu−O)	ΔH_{rel}
0	CH_4	3.6	4.6	*b*	−141.0	56.0	−85.1	6.0	−26.0	104.0	−156.0
1	CH_3F	16.4	−9.2	−49.4	−141.0	45.6	−95.4	11.0	−45.1	102.2	−200.0
2	CH_2F_2	13.4	−7.0	−46.0	−136.4	42.4	−94.0	8.0	−45.2	76.2	−236.6
3	CHF_3	25.4	14.0	−21.1	−112.3	57.7	−54.6	0.5	−25.5	55.4	−236.6

[a]Utilizing B3LYP/TZVP+G(3df,2p):6-311++G(3df,2p). [b]Not calculated.

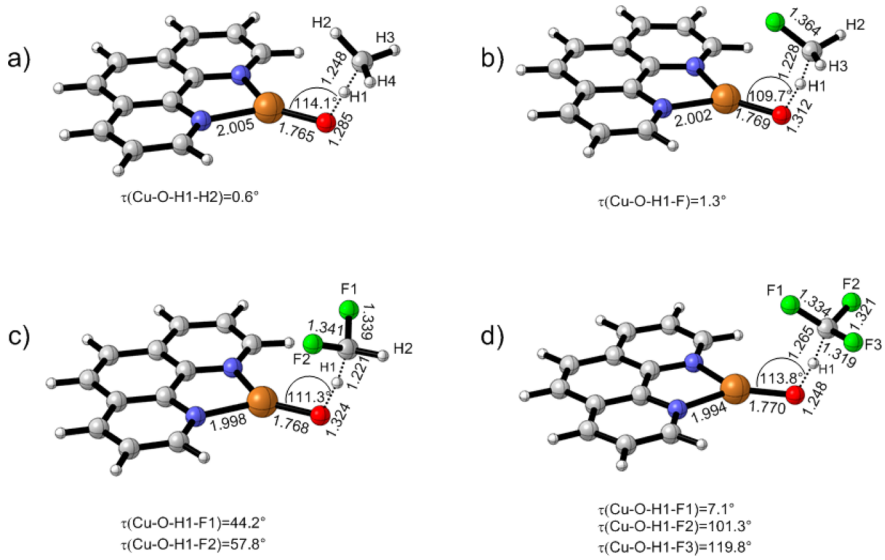

Figure 6. Comparison of TS geometries for direct HAT from (a) CH_4, (b) CH_3F, (c) CH_2F_2, and (d) CHF_3 calculated at the B3LYP/TZVP +G(3df,2p):6-311++G(3df,2p) level. Bond lengths are in angstroms, and angles are in degrees.

important kinetic and thermodynamic differences are observed (Table 2).

The HAT reaction of the ^{3}**1**/CH_2F_2 system is as thermodynamically favorable as the reaction with CH_3F (both exothermic by −45 kJ mol^{-1}; Table 2). The activation energy (E_a) required for HAT to take place is, by comparison, actually slightly lower than that required for monofluoromethane activation. However, the relative energy of CH_2F_2−^{3}TS**4**−**5** is marginally (2.2 kJ mol^{-1}) higher than that of CH_3F−^{3}TS**4**−**5** (n = 2 and 1, respectively; Table 2). Thus, even though the C−H bond activation of difluoromethane is slightly more kinetically hindered, the generation of $CHF_2^{\bullet}$ radicals is predicted to occur under similarly ambient conditions.

Upon overcoming CH_2F_2−^{3}TS**4**−**5**, the system can also pass through an ISC (T → S) regime, giving rise to the methylated copper-hydroxo complex CH_2F_2−^{1}**9** (−136.4 kJ mol^{-1}; Table 2). An MECP has been localized between these two species, located −46 kJ mol^{-1} below the energy of the separated reactants. The formation of the CH_2F_2−^{1}**9** complex is slightly less favorable than the formation of the corresponding CH_3F−^{1}**9** intermediate; nevertheless, the rebound step through ^{1}TS**9**−**6** has an energy barrier of 42.4 kJ mol^{-1}, ∼ 3 kJ mol^{-1} lower than that of the CH_3F system (n = 2 and 1, respectively; Table 2). The formation of the products (^{1}**3** + CHF_2OH) is calculated to be exothermic by 236.3 kJ mol^{-1}, thus outcompeting HF formation in this case as well (Supporting Information, Figure S5).

Whereas the HAT and OAT processes are accessible under thermal conditions for CH_2F_2, the same does not hold true for CHF_3 (n = 3; Table 2), as the relative energy for HAT is 14 kJ mol^{-1} above the energy of the separated reactants and is therefore kinetically prevented under thermal conditions. This is in line with the experimental findings for this system, where no reaction between CDF_3 and ^{3}**1** was observed (Figure 1).

Comparing the Effects of the Degree of Fluorination on the Reactions of ^{3}1 and $CH_{(4-n)}F_n$, n = 0−3. Successful C−H bond activation is determined by an accessible HAT under thermal conditions.[37−42] In the reaction between ^{3}**1** and CH_4 or CHF_3, a lack of reactivity is observed because of the inaccessibility of the corresponding transition states (^{3}TS**4**−**5**), which are 4.6 and 14 kJ mol^{-1}, respectively, above their corresponding separated reactants (Table 2, n = 0 and 3, and Supporting Information, Figures S3 and S6). This trend is in line with the substrates' corresponding trends in C−H bond strengths (Table 1), as well as in the interactions with the copper complex (i.e., the well depth of intermediate **4**).

A comparison of the ^{3}TS**4**−**5** structures for $CH_{(4-n)}F_n$, n = 0−3 (Figure 6), reveals that n = 0 and 3 (i.e., methane and fluoroform; Figure 6a,d) share a structural similarity, namely, a Cu−O−H(1) bond angle of 114°. The two thermally accessible TSs, n = 1 and 2 (mono- and difluoromethane; Figure 6b,c) have tighter Cu−O−H(1) bond angles of 110° and 111°, respectively. Interestingly, the rotation of the methyl group aligns F1 in the plane of bond formation in all cases except for n

DOI: 10.1021/jacs.5b12972
J. Am. Chem. Soc. 2016, 138, 3125−3135

= 2, but this seems to have little bearing on the observed reactivities.

To gain insight into the effects of the degree of fluorination on the bonding and structure during the HAT process, a topological analysis of the electron density within the framework of Bader's quantum theory of atoms in molecules (QTAIM) was carried out.[97] The presence of a (3, −1)-type bond critical point (bcp) indicates interaction. In the transition state ^{3}TS**4**−**5**, no (3, −1) bcp was found between Cu and F; therefore, any organization in the TS results from preorganization in the encounter complex, rather than from Cu−F interaction in the TS geometry. It is thus logical that the kinetic trends in HAT follow those of the C−H bond strength (Table 1).

The entries in Table S1 indicate the cases where interaction with Cu is found for the intermediate complexes. Analysis of the electron density of the fluoromethane encounter complex, ^{3}**4**, for each of the n = 0−3 systems reveals the presence of a (3, −1)-type bcp between Cu and only one F atom (Table S1, entries 1−3). Interestingly, the increase in the degree of fluorination in the substrate (n = 1−3) does not result in an increase in the number of F atoms interacting with the metal center, despite their availability to do so, as no additional (3, −1) bcps between Cu and F were observed. In fact, the stability of the encounter complexes decreases with increased fluorination (the relative energies of ^{3}**4** are 1, −25.6, −20.4, and −11.4 kJ mol^{-1} for n = 0−3, respectively; Supporting Information, Figures S3−S6). The contribution of the ion available for templation (i.e., K^+) would presumably help to counteract the destabilization in the case of fluoroform.[20]

The same effect is revealed for the HAT product complex, ^{3}**5**, where, again, there is only a bonding interaction (i.e., (3, −1) bcp) with one single F atom of each methyl moiety. The stability of the product complexes also decreases with increased fluorination (the relative energies of ^{3}**5** are −32.0, −56.0, −53.2, and −26 kJ mol^{-1} for n = 0−3, respectively; Supporting Information, Figures S3−S6). Thus, the interaction between Cu−F is key in the stability of the radical reactive intermediate ^{3}**5**.

The small value of the electron density [$\rho(r)$] together with a positive value of the Laplacian [$\nabla^2\rho(r)$] and electronic energy density [$H(r)$] indicate a pure closed-shell (i.e., ionic) interaction between F and Cu in both cases (Table S1). As the degree of fluorination increases in both complexes ^{3}**4** and ^{3}**5**, the value of $\rho(r)$ at the (3, −1) bcp decreases in line with the stability of the encounter complexes compared to the stability of the $CH_{(3-n)}F_n^{\bullet}$ radical (Table S1, entries 1−3 and 4−5, respectively). Thus, destabilization of this interaction is brought about by the addition of fluorine. This trend also leads to no bcp being found for ^{3}**5**, n = 3 (Table S1, entry 6). Stabilization through additional ionic templation (such as with additional K cations; e.g., Scheme 1) presumably mitigates this effect in the case of fluoroform activation in the condensed phase. Thus, the radical is "captured" by the noncovalent interaction between F and Cu (or a template ion, such as K) and available for subsequent fluoromethylations.

For n = 0 and 3, HAT is not predicted to occur at room temperature, and as a consequence, OAT is not accessible. However, HAT occurring (i.e., for n = 1 and 2) does not guarantee that OAT will take place. The accessibility of OAT is also mediated by the probability of a change in spin state (T → S), which is, in turn, determined by the spin−orbit coupling (SOC) at the MECP. Comparison of the MECPs for n = 1−3 reveals that they share a striking structural similarity (Figure 7)

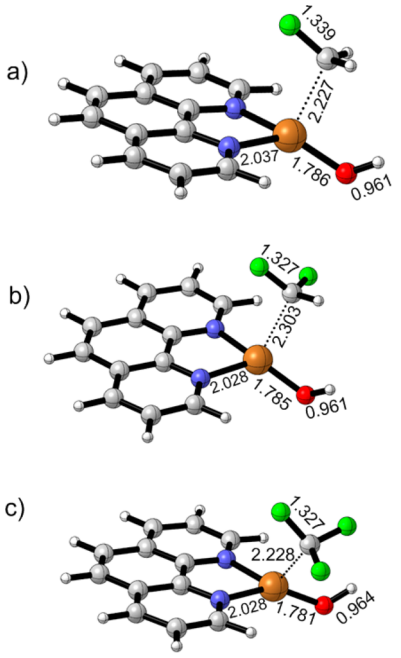

Figure 7. MECPs characterized at the B3LYP level of theory for the reaction of [(phen)CuO]$^+$ with (a) CH_3F, (b) CH_2F_2, and (c) CHF_3 calculated at the B3LYP/TZVP+G(3df,2p):6-311++G(3df,2p) level. Bond lengths are in angstroms.

and, thus, occur in a similar fashion. This is logical, given that, in each case, the spin-crossover process is associated with a change in the coordination sphere, ultimately resulting in square-planar coordination of the closed-shell singlet copper complex ^{1}**9**.

The TSs for the rebound step resulting in an oxidized product (^{1}TS**9**−**6**) are also structurally similar for the various species (e.g., Figure 4 for n = 1, and Supporting Information, Figures S3−S6, for n = 0−3, respectively). However, energetically, there is a change in the associated barrier depending on the substrate (Table 2). The least favorable oxidation, n = 3, has both an increase in the activation barrier (by 10−15 kJ mol^{-1} compared to n = 1 and 2) and a higher relative energy overall, because of the higher-energy square-planar intermediate complex ^{1}**9** (112.3 kJ mol^{-1}; Table 2), as a result of the additional fluorination. Thus, the substrate also kinetically mediates the oxidation process. However, the overall OAT process under the conditions of our experiment is rate-limited by HAT.

Interestingly, no (3, −1) bcp between Cu and F is observed at the fluoromethanol−copper complex, ^{1}**6**, for any of the values n = 1−3. In contrast, a (3, −1) bcp between O and Cu is observed (Table S1, entries 7−9). Small values of the electron density $\rho(r)$, positive values of $\nabla^2\rho(r)$, and negative values of the $H(r)$ indicate a closed-shell interaction, but shifted toward a shared interaction (i.e., with some covalent character). This is also reflected in the larger dissociation energies of $CH_{(3-n)}F_nOH$ [D(Cu−O); Table 2] compared to $CH_{(3-n)}F_n^{\bullet}$ [D(Cu−F); Table 2]. Notably, complex ^{1}**6** bears a structural similarity to the copper fluoromethoxide complexes synthesized by Zhang and Vicic.[98] The in situ formation of fluoromethanols, unstable products (with respect to decomposition) that

DOI: 10.1021/jacs.5b12972
J. Am. Chem. Soc. 2016, 138, 3125−3135

are thermodynamically driven nonetheless by the formation of a very stable closed-shell copper(I) complex, would also play a role as selective reactive intermediates in fluoromethylation reactions, alongside the formation of methyl radicals through HAT.

The copper-catalyzed destruction of the fluoromethyl moiety through ^{1}TS**6**−**11** (Supporting Information, Figures S3−S6) resulting in HF and aldehyde was also explored.[99−103] However, it was found to be kinetically disfavored compared to alcohol dissociation in all three cases (n = 1−3), all having similar activation energies. We note that, in a condensed-phase environment, even though the unimolecular process is disfavored, any water (or HF) present would assist this reaction and hamper the formation of $CH_{(3-n)}F_nOH$. Indeed, even in our gas-phase experiments, the "hot" ions formed as a result of the ion/molecule reaction might be expected to compete to form HF and aldehyde alongside $CH_{(3-n)}F_nOH$ on the time scale of our experiments.

CONCLUSIONS

We have shown that the species ^{3}[(phen)CuO]$^{+}$, as predicted computationally, is capable of activating the C−H bond in CH_3F and CH_2F_2 through HAT under thermal conditions. Products observed for CH_3F result from a combination of HAT and OAT processes. Although HAT is largely determined by the C−H bond strength in the fluoromethane substrate, there is also increased organization in the encounter complex with fluorinated substrates, due to noncovalent interactions between the Cu and F atoms, that helps to organize the activation complex and, in turn, lowers the HAT kinetic barrier in comparison to that of methane. OAT can occur only after HAT has taken place, in the framework of a TSR scenario mediated by the probability of a change in spin state (T → S) determined by the SOC at the MECP. This finding for oxidation reactions is consistent with oxidations of aryl fluoride substrates mediated by ^{3}[(phen)CuO]$^{+}$, which also rely on a T → S spin crossover to take place.[84]

CHF_3 does not show significant reactivity toward C−H bond activation, which is rationalized by a change in kinetic behavior. Other factors that modulate reactivity through a lowering of the TS barrier for HAT, such as addition of a templating ion,[20] would presumably allow this reaction to occur under ambient conditions (e.g., through K^+-promoted stabilization of the encounter complex and lowering of the HAT reaction barrier), as is known to occur during the cupration of fluoroform.

The reactions are completely selective for C−H bond activation; no competing C−F activation was observed.[76] Additionally, no $CuCF_3$-type or analogous complexes were isolated in our experiments. However, the noncovalently bound ion/molecule complex ^{3}**5** is a reactive intermediate consistent with a "coordination-sphere capture" type of a radical intermediate as proposed for complexes of other metals, such as Ag[16] and Ru.[104] We propose that a similar type of $CF_3^{\bullet}$ coordination-sphere-captured radical intermediate might be involved in the K^+-templated reaction of fluoroform.[20]

Given how many fluorinated organic compounds now exist in the biosphere, it will be of interest to see how fluorinated substrates are broken down into metabolites by enzymes; soluble methane monooxygenase has indeed already been shown to break down fluoromethanes into fluoromethanols through HAT.[105]

Whether other analogous metal complexes, such as those of Pd and Ni, are able to mediate such reactivity is also of interest. We intend to publish results on this subject in due course.

EXPERIMENTAL METHODS

Materials and Sample Preparation. Copper nitrate was obtained from Grüssing, CDF_3 from CDN isotopes, and CD_3F and 1,10-phenanthroline from Aldrich. All fluoromethanes were obtained from ABCR GmbH & Co. KG. All chemicals were used as supplied without further purification.

Mass Spectrometry. Experiments were performed on a Synapt-G2 TWIMS time-of-flight (TOF) instrument (Waters, Manchester, U.K.),[106] modified to allow for ion/molecule reactions, as previously described.[84,89] A standard electrospray ionization (ESI) source with a gastight syringe with a sample pump rate of 4 μL/min and a typical source temperature of 100−120 °C was used. The source conditions were tuned to allow for the formation of the copper complexes and were held constant unless otherwise stated. The wave height in the traveling-wave cell was nominally set to 40 V, and the wave velocity was set to 1100 m/s. The mass window (m/z 20−600), gas controls, mass-selected ion (m/z 259), and all other instrument settings were held at the same values for all experiments. The pressures of neutral substrates were measured with specially fitted CMR capacitive gauges.[89] The estimated exposure time to the neutral reagent of 0.57 ms was calculated from the 10-cm length of the transfer cell and a transfer wave velocity of 175 m/s, as per the literature method.[90]

Electronic Structure Calculations. All calculations were carried out with Gaussian 09,[107] utilizing the B3LYP functional. DFT methods were validated against post-Hartree−Fock methods for the reactivity of unligated copper oxide cation with methane by Ugalde and co-workers.[87] Likewise, B3LYP has been found to be in agreement with experimental trends of reactive processes concerning [LCuO]$^+$ (L = 1,10-phenanthroline) derivative species.[81−84] Structures were confirmed to be stationary points by analysis of the vibrational frequencies and the stability of the wave function. Transition states were confirmed by the presence of one negative vibrational frequency, and intrinsic reaction coordinates (IRC) were examined to ensure the smooth connection of reactants to products.[108−110] Zero-point energies were calculated at the level of geometry optimization and are unscaled. All energies presented were calculated with the B3LYP functional, using the 6-311++G(3df,2p)[111] basis set for carbon, oxygen, hydrogen, and fluorine atoms, whereas for the Cu atoms, the all-electron TZVP basis set,[112,113] supplemented with a diffuse s function, two sets of p functions (optimized by Wachters[114]), one set of diffuse pure-d angular-momentum functions (optimized by Hay[115]), and three sets of uncontracted pure-momentum f functions, including both tight and diffuse exponents (as recommended by Raghavachari and Trucks[116]), was used [defined as TZVP+G(3df,2p)].[87,117] Thus, the overall basis set is defined as TZVP+G(3df,2p):6-311++G(3df,2p). Topological analysis of the electron density was performed by applying Bader's quantum theory of atoms in molecules (QTAIM).[97] The program Multiwfn was employed for these purposes.[118]

For those PESs involving TSR,[92−96] along with the stationary points (minima and TSs), regions where the relevant spin states lie close in energy (MECPs) were located. Structures having identical geometries and energies in the singlet and triplet states were calculated by means of the mathematical algorithm for MECPs developed by Harvey et al.[119]

ASSOCIATED CONTENT

Supporting Information

The Supporting Information is available free of charge on the ACS Publications website at DOI: 10.1021/jacs.5b12972.

Additional mass spectra as mentioned in the text. Potential energy surfaces of CH_4, CH_3F, CH_2F_2, and CHF_3. Additional discussion as mentioned in the text. Cartesian coordinates and transition-state frequencies for all calculated species (PDF)

DOI: 10.1021/jacs.5b12972
J. Am. Chem. Soc. 2016, 138, 3125−3135

AUTHOR INFORMATION

Corresponding Authors

*Helmut.Schwarz@tu-berlin.de
*nicole.rijs@kit.edu

Notes

The authors declare no competing financial interest.

ACKNOWLEDGMENTS

N.J.R. and P.G.-N. thank the Alexander von Humboldt foundation for support in the form of postdoctoral fellowships. Generous funding by the Deutsche Forschungsgemeinschaft ("UniCat" Cluster of Excellence) and the Fonds der Chemischen Industrie is appreciated. We also thank Dr. Fernando Ruipérez for providing the modified basis set for copper and Dr. Thomas Weiske for technical assistance. This article is dedicated to Professor Harry B. Gray on the occasion of his 80th birthday.

REFERENCES

(1) *Organofluorine Chemistry: Principles and Commercial Applications*; Banks, R. E., Smart, B. E., Tatlow, J., Eds.; Springer Science & Business Media: New York, 1994.
(2) Hiyama, T. *Organofluorine Compounds: Chemistry and Applications*; Springer-Verlag: Heidelberg, Germany, 2000.
(3) Kirsh, P. *Modern Fluoroorganic Chemistry: Synthesis, Reactivity, Applications*; Wiley-VCH: Weinheim, Germany, 2004.
(4) Uneyama, K. *Organofluorine Chemistry*; Blackwell: Oxford, U.K., 2006.
(5) Purser, S.; Moore, P. R.; Swallow, S.; Gouverneur, V. *Chem. Soc. Rev.* **2008**, *37*, 320−330.
(6) O'Hagan, D. *Chem. Soc. Rev.* **2008**, *37*, 308−319.
(7) Shibata, N.; Matsnev, A.; Cahard, D. *Beilstein J. Org. Chem.* **2010**, *6*, 65.
(8) Ma, J.-A.; Cahard, D. *J. Fluorine Chem.* **2007**, *128*, 975−996.
(9) McClinton, M. A.; McClinton, D. A. *Tetrahedron* **1992**, *48*, 6555−6666.
(10) McReynolds, K. A.; Lewis, R. S.; Ackerman, L. K. G.; Dubinina, G. G.; Brennessel, W. W.; Vicic, D. A. *J. Fluorine Chem.* **2010**, *131*, 1108−1112.
(11) Tomashenko, O. A.; Grushin, V. V. *Chem. Rev.* **2011**, *111*, 4475−4521.
(12) Prakash, G. K. S.; Jog, P. V.; Batamack, P. T. D.; Olah, G. A. *Science* **2012**, *338*, 1324−1327.
(13) Ye, Y.; Sanford, M. S. *J. Am. Chem. Soc.* **2012**, *134*, 9034−9037.
(14) Ye, Y.; Sanford, M. S. *Synlett* **2012**, *23*, 2005−2013.
(15) Ye, Y.; Kuenzi, S. A.; Sanford, M. S. *Org. Lett.* **2012**, *14*, 4979−4981.
(16) Ye, Y.; Lee, S. H.; Sanford, M. S. *Org. Lett.* **2011**, *13*, 5464−5467.
(17) Novak, P.; Lishchynskyi, A.; Grushin, V. V. *Angew. Chem., Int. Ed.* **2012**, *51*, 7767−7770.
(18) Zanardi, A.; Novikov, M. A.; Martin, E.; Benet-Buchholz, J.; Grushin, V. V. *J. Am. Chem. Soc.* **2011**, *133*, 20901−20913.
(19) Nebra, N.; Grushin, V. V. *J. Am. Chem. Soc.* **2014**, *136*, 16998−17001.
(20) Konovalov, A. I.; Benet-Buchholz, J.; Martin, E.; Grushin, V. V. *Angew. Chem., Int. Ed.* **2013**, *52*, 11637−11641.
(21) Limberg, C. *Angew. Chem., Int. Ed.* **2003**, *42*, 5932−5954.
(22) Fokin, A. A.; Schreiner, P. R. *Chem. Rev.* **2002**, *102*, 1551−1593.
(23) Shilov, A. E.; Shul'pin, G. B. *Chem. Rev.* **1997**, *97*, 2879−2932.
(24) Shiota, Y.; Yoshizawa, K. *J. Am. Chem. Soc.* **2000**, *122*, 12317−12326.
(25) Haack, P.; Limberg, C. *Angew. Chem., Int. Ed.* **2014**, *53*, 4282−4293.
(26) Company, A.; Lloret, J.; Gomez, L.; Costas, M. In *Alkane C−H Activation by Single-Site Metal Catalysis*; Pérez, P. J., Ed.; Springer: Dordrecht, The Netherlands, 2012; Vol. *38*, section 5.7, pp 190−195.
(27) Smeets, P. J.; Hadt, R. G.; Woertink, J. S.; Vanelderen, P.; Schoonheydt, R. A.; Sels, B. F.; Solomon, E. I. *J. Am. Chem. Soc.* **2010**, *132*, 14736−14738.
(28) Woertink, J. S.; Smeets, P. J.; Groothaert, M. H.; Vance, M. A.; Sels, B. F.; Schoonheydt, R. A.; Solomon, E. I. *Proc. Natl. Acad. Sci. U. S. A.* **2009**, *106*, 18908−18913.
(29) Groothaert, M. H.; Smeets, P. J.; Sels, B. F.; Jacobs, P. A.; Schoonheydt, R. A. *J. Am. Chem. Soc.* **2005**, *127*, 1394−1395.
(30) Kirillov, A. M.; Kopylovich, M. N.; Kirillova, M. V.; Haukka, M.; da Silva, M.; Pombeiro, A. J. L. *Angew. Chem., Int. Ed.* **2005**, *44*, 4345−4349.
(31) Nagababu, P.; Yu, S. S. F.; Maji, S.; Ramu, R.; Chan, S. I. *Catal. Sci. Technol.* **2014**, *4*, 930−935.
(32) Chen, P. P. Y.; Nagababu, P.; Yu, S. S. F.; Chan, S. I. *ChemCatChem* **2014**, *6*, 429−437.
(33) Baber, A. E.; Xu, F.; Dvorak, F.; Mudiyanselage, K.; Soldemo, M.; Weissenrieder, J.; Senanayake, S. D.; Sadowski, J. T.; Rodriguez, J. A.; Matolín, V.; White, M. G.; Stacchiola, D. J. *J. Am. Chem. Soc.* **2013**, *135*, 16781−16781.
(34) Hammond, C.; Jenkins, R. L.; Dimitratos, N.; Lopez-Sanchez, J. A.; ab Rahim, M. H.; Forde, M. M.; Thetford, A.; Murphy, D. M.; Hagen, H.; Stangland, E. E.; Moulijn, J. M.; Taylor, S. H.; Willock, D. J.; Hutchings, G. J. *Chem. - Eur. J.* **2012**, *18*, 15735−15745.
(35) Palomas, D.; Kalamaras, C.; Haycock, P.; White, A. J. P.; Hellgardt, K.; Horton, A.; Crimmin, M. R. *Catal. Sci. Technol.* **2015**, *5*, 4108−4115.
(36) Balasubramanian, R.; Smith, S. M.; Rawat, S.; Yatsunyk, L. A.; Stemmler, T. L.; Rosenzweig, A. C. *Nature* **2010**, *465*, 115−119.
(37) Schwarz, H. *Chem. Phys. Lett.* **2015**, *629*, 91−101.
(38) Schwarz, H. *Isr. J. Chem.* **2014**, *54*, 1413−1431.
(39) Schwarz, H. *Angew. Chem., Int. Ed.* **2011**, *50*, 10096−10115.
(40) Schlangen, M.; Schwarz, H. *Dalton Trans.* **2009**, 10155−10165.
(41) Schröder, D.; Schwarz, H. *Proc. Natl. Acad. Sci. U. S. A.* **2008**, *105*, 18114−18119.
(42) Schröder, D.; Schwarz, H. *Angew. Chem., Int. Ed. Engl.* **1995**, *34*, 1973−1995.
(43) Li, J.; Wu, X.-N.; Zhou, S.; Tang, S.; Schlangen, M.; Schwarz, H. *Angew. Chem., Int. Ed.* **2015**, *54*, 12298−12302.
(44) Li, J.; Wu, X.-N.; Schlangen, M.; Zhou, S.; González-Navarrete, P.; Tang, S.; Schwarz, H. *Angew. Chem., Int. Ed.* **2015**, *54*, 5074−5078.
(45) Li, J.; González-Navarrete, P.; Schlangen, M.; Schwarz, H. *Chem. - Eur. J.* **2015**, *21*, 7780−7789.
(46) Wang, Z.-C.; Liu, J.-W.; Schlangen, M.; Weiske, T.; Schröder, D.; Sauer, J.; Schwarz, H. *Chem. - Eur. J.* **2013**, *19*, 11496−11501.
(47) Kretschmer, R.; Schlangen, M.; Schwarz, H. *Angew. Chem., Int. Ed.* **2013**, *52*, 6097−6097−6101.
(48) Dietl, N.; Wende, T.; Chen, K.; Jiang, L.; Schlangen, M.; Zhang, X.; Asmis, K. R.; Schwarz, H. *J. Am. Chem. Soc.* **2013**, *135*, 3711−3271.
(49) Dietl, N.; Troiani, A.; Schlangen, M.; Ursini, O.; Angelini, G.; Apeloig, Y.; de Petris, G.; Schwarz, H. *Chem. - Eur. J.* **2013**, *19*, 6662−6669.
(50) Wang, Z.-C.; Dietl, N.; Kretschmer, R.; Ma, J.-B.; Weiske, T.; Schlangen, M.; Schwarz, H. *Angew. Chem., Int. Ed.* **2012**, *51*, 3703−3707.
(51) Ma, J.-B.; Wang, Z.-C.; Schlangen, M.; He, S.-G.; Schwarz, H. *Angew. Chem., Int. Ed.* **2012**, *51*, 5991−5994.
(52) Lakuntza, O.; Matxain, J. M.; Ruiperez, F.; Besora, M.; Maseras, F.; Ugalde, J. M.; Schlangen, M.; Schwarz, H. *Phys. Chem. Chem. Phys.* **2012**, *14*, 9306−9310.
(53) Dietl, N.; Schlangen, M.; Schwarz, H. *Angew. Chem., Int. Ed.* **2012**, *51*, 5544−5555.
(54) Wang, L.-N.; Zhou, Z.-X.; Li, X.-N.; Ma, T.-M.; He, S.-G. *Chem. - Eur. J.* **2015**, *21*, 6957−6961.
(55) Li, H.-F.; Li, Z.-Y.; Liu, Q.-Y.; Li, X.-N.; Zhao, Y.-X.; He, S.-G. *J. Phys. Chem. Lett.* **2015**, *6*, 2287−2291.

DOI: 10.1021/jacs.5b12972
J. Am. Chem. Soc. 2016, 138, 3125−3135

(56) Ding, X.-L.; Wang, D.; Wu, X.-N.; Li, Z.-Y.; Zhao, Y.-X.; He, S.-G. *J. Chem. Phys.* **2015**, *143*, 124312-1−124312-11.
(57) Zhao, Y.-X.; Li, Z.-Y.; Yuan, Z.; Li, X.-N.; He, S.-G. *Angew. Chem., Int. Ed.* **2014**, *53*, 9482−9486.
(58) Wu, X.-N.; Ding, X.-L.; Li, Z.-Y.; Zhao, Y.-X.; He, S.-G. *J. Phys. Chem. C* **2014**, *118*, 24062−24071.
(59) Campbell, M. G.; Ritter, T. *Chem. Rev.* **2015**, *115*, 612−633.
(60) Liang, T.; Neumann, C. N.; Ritter, T. *Angew. Chem., Int. Ed.* **2013**, *52*, 8214−8264.
(61) Furuya, T.; Kamlet, A. S.; Ritter, T. *Nature* **2011**, *473*, 470−477.
(62) Rijs, N. J.; Yoshikai, N.; Nakamura, E.; O'Hair, R. A. J. *J. Am. Chem. Soc.* **2012**, *134*, 2569−2580.
(63) Norinder, J.; Backvall, J. E.; Yoshikai, N.; Nakamura, E. *Organometallics* **2006**, *25*, 2129−2132.
(64) Van Leeuwen, P. W. N. M.; Chadwick, J. C. *Homogeneous Catalysis: Activity−Stability−Deactivation*; Wiley-VCH: Weinheim, Germany, 2011.
(65) Tsang, A. S. K.; Sanhueza, I. A.; Schoenebeck, F. *Chem. - Eur. J.* **2014**, *20*, 16432−16441.
(66) Roithova, J.; Schröder, D. *Coord. Chem. Rev.* **2009**, *253*, 666−677.
(67) Schlangen, M.; Schwarz, H. *Catal. Lett.* **2012**, *142*, 1265−1278.
(68) O'Hair, R. A. J.; Rijs, N. J. *Acc. Chem. Res.* **2015**, *48*, 329−340.
(69) Tsybizova, A.; Roithová, J. *Mass Spectrom. Rev.* **2016**, *35*, 85−110.
(70) O'Hair, R. A. J. *Int. J. Mass Spectrom.* **2015**, *377*, 121−129.
(71) Schröder, D. *Acc. Chem. Res.* **2012**, *45*, 1521−1532.
(72) O'Hair, R. A. J. *Chem. Commun.* **2006**, 1469−1481.
(73) Bizet, V.; Besset, T.; Ma, J.-A.; Cahard, D. *Curr. Top. Med. Chem.* **2014**, *14*, 901−940.
(74) Landelle, G.; Panossian, A.; Pazenok, S.; Vors, J.-P.; Leroux, F. R. *Beilstein J. Org. Chem.* **2013**, *9*, 2476−2536.
(75) Hu, J.; Zhang, W.; Wang, F. *Chem. Commun.* **2009**, 7465−7478.
(76) Mazurek, U.; Schwarz, H. *Chem. Commun.* **2003**, 1321−1326.
(77) Rijs, N. J.; O'Hair, R. A. J. *Dalton Trans.* **2012**, *41*, 3395−3406.
(78) Dau, P. D.; Gibson, J. K. *J. Phys. Chem. A* **2015**, *119*, 3218−3224.
(79) Wang, H.; Vicic, D. A. *Synlett* **2013**, *24*, 1887−1898.
(80) Dubinina, G. G.; Furutachi, H.; Vicic, D. A. *J. Am. Chem. Soc.* **2008**, *130*, 8600−8601.
(81) Shaffer, C. J.; Schröder, D.; Gütz, C.; Lützen, A. *Angew. Chem., Int. Ed.* **2012**, *51*, 8097−8100.
(82) Jašíková, L.; Hanikýřová, E.; Schröder, D.; Roithová, J. *J. Mass Spectrom.* **2012**, *47*, 460−465.
(83) Schröder, D.; Holthausen, M. C.; Schwarz, H. *J. Phys. Chem. B* **2004**, *108*, 14407−14416.
(84) Rijs, N. J.; Weiske, T.; Schlangen, M.; Schwarz, H. *Chem. Phys. Lett.* **2014**, *608*, 408−424.
(85) Methane reactivity studies repeated with TWIMS isomer separated $[(phen)CuO]^+$ confirmed this finding.
(86) Dietl, N.; van der Linde, C.; Schlangen, M.; Beyer, M. K.; Schwarz, H. *Angew. Chem., Int. Ed.* **2011**, *50*, 4966−4969.
(87) Rezabal, E.; Ruiperez, F.; Ugalde, J. M. *Phys. Chem. Chem. Phys.* **2013**, *15*, 1148−1153.
(88) Tang, S.-Y.; Rijs, N. J.; Li, J.; Schlangen, M.; Schwarz, H. *Chem. - Eur. J.* **2015**, *21*, 8483−8490.
(89) Rijs, N. J.; Weiske, T.; Schlangen, M.; Schwarz, H. *Anal. Chem.* **2015**, *87*, 9769−9776.
(90) Ruotolo, B. T.; Benesch, J. L. P.; Sandercock, A. M.; Hyung, S.-J.; Robinson, C. V. *Nat. Protoc.* **2008**, *3*, 1139−1152.
(91) Luo, Y. R.,*Comprehensive Handbook of Chemical Bond Energies*; CRC Press: Boca Raton, FL, 2007.
(92) Harvey, J. N. *WIREs Comput. Mol. Sci.* **2014**, *4*, 1−14.
(93) Schwarz, H. *Int. J. Mass Spectrom.* **2004**, *237*, 75−105.
(94) Schröder, D.; Shaik, S.; Schwarz, H. *Acc. Chem. Res.* **2000**, *33*, 139−145.
(95) Armentrout, P. B. *Science* **1991**, *251*, 175−179.
(96) Armentrout, P. B. *Annu. Rev. Phys. Chem.* **1990**, *41*, 313−344.
(97) Bader, R. F. W. *Atoms in Molecules: A Quantum Theory*; Oxford University Press: New York, 1994.
(98) Zhang, C.-P.; Vicic, D. A. *Organometallics* **2012**, *31*, 7812−7815.
(99) Long, B.; Tan, X.-f.; Ren, D.-s.; Zhang, W.-j. *Chem. Phys. Lett.* **2010**, *492*, 214−219.
(100) Buszek, R. J.; Francisco, J. S. *J. Phys. Chem. A* **2009**, *113*, 5333−5337.
(101) Nguyen, M. T.; Matus, M. H.; Ngan, V. T.; Haiges, R.; Christe, K. O.; Dixon, D. A. *J. Phys. Chem. A* **2008**, *112*, 1298−1312.
(102) Christe, K. O.; Hegge, J.; Hoge, B.; Haiges, R. *Angew. Chem.* **2007**, *119*, 6267−6270.
(103) Schneider, W. F.; Wallington, T. J.; Huie, R. E. *J. Phys. Chem.* **1996**, *100*, 6097−6103.
(104) Kamigata, N.; Ohtsuka, T.; Fukushima, T.; Yoshida, M.; Shimizu, T. *J. Chem. Soc., Perkin Trans. 1* **1994**, 1339−1346.
(105) Beauvais, L. G.; Lippard, S. J. *Biochem. Biophys. Res. Commun.* **2005**, *338*, 262−266.
(106) Giles, K.; Pringle, S. D.; Worthington, K. R.; Little, D.; Wildgoose, J. L.; Bateman, R. H. *Rapid Commun. Mass Spectrom.* **2004**, *18*, 2401−2414.
(107) Frisch, M. J.; Trucks, G. W.; Schlegel, H. B.; Scuseria, G. E.; Robb, M. A.; Cheeseman, J. R.; Scalmani, G.; Barone, V.; Mennucci, B.; Petersson, G. A.; Nakatsuji, H.; Caricato, M.; Li, X.; Hratchian, H. P.; Izmaylov, A. F.; Bloino, J.; Zheng, G.; Sonnenberg, J. L.; Hada, M.; Ehara, M.; Toyota, K.; Fukuda, R.; Hasegawa, J.; Ishida, M.; Nakajima, T.; Honda, Y.; Kitao, O.; Nakai, H.; Vreven, T.; Montgomery, J. A., Jr.; Peralta, J. E.; Ogliaro, F.; Bearpark, M.; Heyd, J. J.; Brothers, E.; Kudin, K. N.; Staroverov, V. N.; Keith, T.; Kobayashi, R.; Normand, J.; Raghavachari, K.; Rendell, A.; Burant, J. C.; Iyengar, S. S.; Tomasi, J.; Cossi, M.; Rega, N.; Millam, J. M.; Klene, M.; Knox, J. E.; Cross, J. B.; Bakken, V.; Adamo, C.; Jaramillo, J.; Gomperts, R.; Stratmann, R. E.; Yazyev, O.; Austin, A. J.; Cammi, R.; Pomelli, C.; Ochterski, J. W.; Martin, R. L.; Morokuma, K.; Zakrzewski, V. G.; Voth, G. A.; Salvador, P.; Dannenberg, J. J.; Dapprich, S.; Daniels, A. D.; Farkas, Ö.; Foresman, J. B.; Ortiz, J. V.; Cioslowski, J.; Fox, D. J. *Gaussian 09*, revision D.01; Gaussian Inc.: Wallingford, CT, 2010.
(108) Fukui, K. *Acc. Chem. Res.* **1981**, *14*, 363−368.
(109) Hratchian, H. P.; Schlegel, H. B. *J. Chem. Theory Comput.* **2005**, *1*, 61−69.
(110) Hratchian, H. P.; Schlegel, H. B. *J. Chem. Phys.* **2004**, *120*, 9918−9924.
(111) Krishnan, R.; Binkley, J. S.; Seeger, R.; Pople, J. A. *J. Chem. Phys.* **1980**, *72*, 650−654.
(112) Schafer, A.; Huber, C.; Ahlrichs, R. *J. Chem. Phys.* **1994**, *100*, 5829−5835.
(113) Schafer, A.; Horn, H.; Ahlrichs, R. *J. Chem. Phys.* **1992**, *97*, 2571−2577.
(114) Wachters, A. J. *J. Chem. Phys.* **1970**, *52*, 1033−1036.
(115) Hay, P. J. *J. Chem. Phys.* **1977**, *66*, 4377−4384.
(116) Raghavachari, K.; Trucks, G. W. *J. Chem. Phys.* **1989**, *91*, 1062−1065.
(117) Irigoras, A.; Elizalde, O.; Silanes, I.; Fowler, J. E.; Ugalde, J. M. *J. Am. Chem. Soc.* **2000**, *122*, 114−122.
(118) Lu, T.; Chen, F. *J. Comput. Chem.* **2012**, *33*, 580−592.
(119) Harvey, J. N.; Aschi, M.; Schwarz, H.; Koch, W. *Theor. Chem. Acc.* **1998**, *99*, 95−99.

DOI: 10.1021/jacs.5b12972
J. Am. Chem. Soc. 2016, 138, 3125−3135